Novel therapeutic potential in targeting microtubules by nanoparticle albumin-bound paclitaxel in hepatocellular carcinoma

QIAN ZHOU[1], ARTHUR K.-K. CHING[2,4], WILSON K.-C. LEUNG[2,4], CAROL Y.-Y. SZETO[5], SHUK-MEI HO[5], PAUL K.-S. CHAN[6], YUN-FEI YUAN[7], PAUL B.-S. LAI[3], WINNIE YEO[1] and NATHALIE WONG[2,4]

Departments of [1]Clinical Oncology, [2]Anatomical and Cellular Pathology at the Li Ka-Shing Institute of Health Sciences, and [3]Surgery, [4]State Key Laboratory in Oncology in South China, Chinese University of Hong Kong, Shatin, Hong Kong, P.R. China; [5]Department of Environmental Health, University of Cincinnati Medical Center, Cincinnati, OH, USA; [6]Department of Microbiology, Centre for Emerging Infectious Diseases, School of Public Health, Chinese University of Hong Kong, Shatin, N.T., Hong Kong SAR; [7]State Key Laboratory in Oncology in South China and Department of Hepatobiliary Surgery, Sun Yat-sen University Cancer Center, Guangzhou, P.R. China

Received August 10, 2010; Accepted October 12, 2010

DOI: 10.3892/ijo.2011.902

Abstract. Hepatocellular carcinoma (HCC) shows low response to most conventional chemotherapies. To facilitate target identification for novel therapeutic development, we deployed gene expression profiling on 43 paired HCC tumors and adjacent non-tumoral liver, which is also considered as the pre-malignant liver lesion. In conjunction with ontology analysis, a major functional process found to play a role in the malignant transformation of HCC was microtubule-related cellular assembly. We further examined the potential use of microtubule targeting taxane drugs, including paclitaxel and docetaxel, and compared with findings to results from doxorubicin, a common chemotherapeutic agent used in HCC. Recent studies showed that drug delivery by nanoparticles have enhanced efficacy with reduced side effects. In this regard, the nanoparticle albumin-bound (*nab*)-paclitaxel was also examined. In a panel of HCC cell lines studied, a high sensitivity towards taxane drugs was generally found, although the effect from *nab*-paclitaxel was most profound. The *nab*-paclitaxel showed an effective IC_{50} dose at 15-fold lower than paclitaxel alone or the derivative analogue docetaxel, and ~450-fold less compared to doxorubicin. Flow cytometric analysis confirmed a cell cycle blockade at the G_2/M phase and increased apoptosis following *nab*-paclitaxel treatment. *In vivo* animal studies also showed that *nab*-paclitaxel readily inhibited xenograft growth with less toxicity to host cells compared to other anti-microtubule drugs and doxorubicin. Gene silencing of the microtubule regulatory gene STMN1 by RNAi suggested a distinct synergistic effect in the combined treatment with *nab*-paclitaxel. Our findings in this study highly suggest that the microtubule assembly represents a promising therapeutic target development in HCC.

Correspondence to: Dr Nathalie Wong, Department of Anatomical and Cellular Pathology, The Chinese University of Hong Kong, Prince of Wales Hospital, Shatin, N.T., Hong Kong, P.R. China
E-mail: natwong@cuhk.edu.hk

Abbreviations: AJCC, American Joint Committee on Cancer; SAM, significance analysis of microarray; FDR, false discovery c saline; MTT, 3-(4,5-dimethylthiazol-2-yl)-2,5-diphenyl tetrazolium bromide; DAPI, 4, 6-diaminidino-2-phenylindole; SDS-PAGE, sodium dodecyl sulfate-polyacrylamide gel electrophoresis

Key words: hepatocellular carcinoma, *nab*-paclitaxel, STMN1, expression array, therapy

Introduction

Hepatocellular carcinoma (HCC) is the fifth most common cancer worldwide and the third most common cause of cancer-related deaths annually (1). The dismal outcome of individuals diagnosed with HCC is largely attributed to the disease being often diagnosed late in the course of clinical manifestation. As a result, only 10-15% of patients are candidates for curative surgery. For the majority of HCC patients, systemic chemotherapies or supportive therapies are the mainstay treatment options. Nevertheless, most chemotherapeutic agents show limited effectiveness and have not been able to improve patient survival (2-5). Recent Phase III randomized trial of Sorafenib, an oral multi-kinase inhibitor of the VEGF receptor, PDGF receptor, and Raf, on hepatitis B-related HCC patients showed for the first time to prolong survival of advanced stage patients (6). However, the median overall survival barely increased from 4.2 months in the placebo group to 6.5 months in the treatment group (6). Moreover, HCC are inherently chemotherapy-resistant tumors and are known to over-express multi-drug resistance genes, such as MDR1 (P-gp) and the multi-drug resistance proteins (MRPs) (7-9). The adverse clinical course of most HCC patients underscores the need for more

efficacious chemotherapies and development of targeting strategies.

Gene expression profiling has led to the discovery of vital signaling paths in human oncogenesis, and aided identifications of molecular targets for therapeutic developments. Using this approach, a number of potential targets such as extra-cellular matrix (ECM) related genes, osteopontin, fatty acid-binding protein 7 (FABP7), serine/threonine kinase 31 (STK31) have been previously suggested in breast cancer, colorectal cancer, melanoma, glioblastoma and gastrointestinal cancer (10-14). In this study, we carried out gene expression profiling in conjunction with ontology analysis to decipher functional changes that underlie the malignant transformation of HCC. A number of aberrant pathways were suggested, amongst which deregulations of microtubule-related cellular assembly ranked the most significant.

Based on the annotation results obtained from Gene Ontology, we explored the potential use of microtubule targeting drugs for their therapeutic utility in HCC cells. Microtubule-binding agents (taxanes) are a class of diterpenoid drugs (15) that have anti-tumor activity against a wide range of human cancers (16-18). Paclitaxel is the most commonly used taxane, while docetaxel is a synthetic taxoid structurally similar to paclitaxel. However, both have low aqueous solubility requiring solubilization with surfactants and solvents and show treatment associated severe toxicity in patients (19,20). Nanoparticle albumin-bound (*nab*)-paclitaxel is a 130-nm particle formulation of paclitaxel that is devoid of any surfactant, solvent or ethanol carriers (21). *nab*-paclitaxel has been shown to exert high anti-tumor activity, more effective intratumoral accumulation and less cytotoxicity than paclitaxel in pre-clinical animal models of multiple cancers (22,23). In this study, we investigated the comparative anti-tumor activity of taxane-based drugs and doxorubicin in HCC cell lines and xenograft model. We also examined the efficacy of taxanes in combination with silencing of Stathmin1 (STMN1), a key regulatory protein that controls the microtubule dynamics.

Materials and methods

Expression profiling and informatic analysis. Gene expression profiling on 43 paired HCC tumors and adjacent non-tumoral livers was performed according to method previously described (24). Demographic information of cases studied is shown in Table I. Normal liver RNA from three individuals were pooled and used as reference control in array hybridisation (Ambion, Austin, TX; Clontech Laboratory Inc., Palo Alto, CA; and Strategene, La Jolla, CA). Briefly, reverse-transcribed RNA from test sample and normal liver pool were differentially labelled with fluorescent Cy5-dCTP or Cy3-dCTP. Labelled cDNAs were co-hybridised onto 19K cDNA arrays (Ontario Cancer Institute, Canada). Hybridised signals captured by ScanArray 5000 (Packard BioScience, UK) were analysed by GenePix Pro4.0 (Axon, CA). Results from duplicate spots and dye swap experiments were averaged, and the normalized intensity ratio for each transcript was subjected to informatic analysis to determine the influential genes involved in the malignant HCC transformation.

A combined parametric and non-parametric analysis was performed on the microarray profiles obtained. Statistical significance (P-value) for each gene is calculated based on a pair-wise permutation t-test using significant analysis for microarray (SAM) and paired Wilcoxon signed rank test. Correction for multiple hypotheses testing has also been carried out using Bonferonni or false discovery rate analysis. To establish the significance of a gene, the combined P-value from SAM and Wilcoxon tests was averaged, and scored for precedence by ranking. Genes that ranked top 5% percentile (at ≥2.0-fold median up- or down-regulation) were selected and further subjected to functional ontology analysis by Ingenuity Pathway Analysis (IPA; http://www.ingenuity.com).

Cell culture and taxane drugs. Human liver cancer cell lines Hep3B and SK-HEP-1 acquired from ATCC were cultured in Dulbecco's modified Eagle's medium with Glutamax-1 (Gibco-BRL, Grand Island, NY, USA) supplemented with 10% fetal bovine serum. HKCl-9 previously established from our group (25) was cultured in AIMV medium (Gibco-BRL) supplemented with 1% L-glutamine and 10% fetal bovine serum. All cells were cultured under a humidified atmosphere of 5% CO_2 at 37˚C.

Doxorubicin was purchased from EBEWE Pharma Ges (Unterach, Austria), and stored at a concentration of 2 mg/ml at 4˚C. Paclitaxel (Taxol®) was obtained from Bristol-Myers Squibb (Princeton, NJ, USA), and stored at a concentration of 6 mg/ml in 527 mg of purified Cremophor® EL and 49.7% dehydrated alcohol at -20˚C. Docetaxel (Taxotere®) was obtained from Aventis Pharma SA (Paris, France), and stored at a concentration of 10 mg/ml in 13% w/w ethanol at 4˚C. The nanoparticle albumin-bound (*nab*)-paclitaxel (*nab*-paclitaxel, Abraxane®) was obtained from Abraxis BioScience (Los Angeles, CA, USA). Each vial of *nab*-paclitaxel supplied contains 100 mg of paclitaxel, stabilized in 900 mg of albumin. Upon reconstitution, 20 ml of PBS was added to give a stock concentration of 5 mg/ml *nab*-paclitaxel and stored at -20˚C until use.

Cell viability assay. Cell viability was measured by MTT assay. Cells grown in 96-well plates at density of 3000 cells per well were treated with drugs or siRNA transfection as indicated. Paclitaxel, docetaxel and *nab*-paclitaxel were tested at different concentrations ranging from 0 to 40 μg/ml for 48 h, while doxorubicin tested at concentrations ranging from 0 to 150 μg/ml for 48 h. The formazan formed was measured at 570 nm and cell viability expressed as a percentage of maximum absorbance from 5 replicates in 3 independent experiments. The concentration of drug that inhibited cell survival by 50% (IC_{50}) was determined from cell survival curves.

Immunofluorescence analysis. Cells plated on sterile 18x18 mm glass cover slip was allowed to adhere for 24 h prior to treatment with 5 ng/ml *nab*-paclitaxel or medium for another 24 h. Cells fixed in 4% paraformaldehyde were then incubated with anti-ß-tubulin (Zymed, Invitrogen) at 1:100 dilution. Secondary antibody Alexa-598-coupled anti-mouse immunoglobulin (Molecular Probes, Eugene, OR, USA) was applied at 1:200 dilution. Cell nuclei counterstained in DAPI (Molecular Probes) were examined under a fluorescence microscope (Nikon EFD-3, Japan). Post-capture image analysis and

Table I. Demographic information of 43 HCC patients studied by gene expression profiling.

	HCC patients (n=43)
Gender	
Male	35 (81.4%)
Female	8 (18.6%)
Age	
Median (quartiles)	58 (50-67)
HbsAg	
Positive	40 (93.0%)
Negative	3 (7.0%)
Underlying liver cirrhosis	
Present	37 (86.0%)
Absent	6 (14.0%)
AJCC Staging	
Stage T1	6 (14.0%)
Stage T2	23 (53.5%)
Stage T3	10 (23.3%)
Stage T4	4 (9.3%)
No. of lesions at presentation	
Single	27 (62.8%)
Multiple	16 (37.2%)

processing of image stacks were performed using the analySIS software.

Flow cytometry analysis of cell cycle. Cell cycle distribution was measured after exposure to different concentrations of *nab*-paclitaxel. After 12 h, all cells including detached cells were harvested and fixed in 70% ethanol at 4˚C overnight. Fixed cells were incubated with RNase A and propidium iodide prior to flow cytometric analysis (BD FACSCalibur™, Becton-Dickinson). The average value of G_0-G_1, S and G_2-M phases were calculated from 2 independent experiments.

TUNEL assay. TUNEL assay was conducted according to procedures of *In Situ* Cell Death Detection Kit (Roche Applied Science, Mannheim, Germany). In brief, cells treated with different concentrations of *nab*-paclitaxel were fixed and incubated with TUNEL reaction mixture for 1 h at 37˚C. Cell nuclei counterstained in DAPI were examined by fluorescence microscope (Nikon EFD-3, Japan). Percentage apoptotic cells were calculated based on at least four randomly fields, which totaled ~200 cells.

siRNA transfection. siRNA sequences, empirically designed based on recommendations of Dharmacon RNA Technologies (Lafayette, CO, USA), included STMN1 si*GENOME SMART*pool (siSTMN1) and si*CONTROL* Non-Targeting siRNA (siMock). All siRNAs were chemically synthesized as double stranded RNA (Dharmacon) and introduced into cell lines by Lipofectamine 2000 (Invitrogen, Carlsbad, CA, USA) according to the manufacturer's instructions. Briefly, cells were incubated with 100 nM siRNA (siSTMN1 or siMock). Six hours after transfection, medium was replaced by fresh growing medium. The expression of STMN1 was monitored by Western blotting, which indicated a repressed expression for at least 3 days. Paclitaxel and *nab*-paclitaxel at concentrations ranging from 0 to 40 μg/ml were applied at 6th hour after siRNA transfections. MTT assay for cell viability was carried out at 48 h, and the IC_{50} values calculated as described.

Immunoblotting. Protein lysates from cells treated with *nab*-paclitaxel for 48 h and untreated control cells were quantified using the Bradford Protein Assay (Bio-Rad Laboratories, Hercules, CA, USA). Equal amounts of protein lysates (30-60 μg) were separated by SDS-PAGE and electrotransferred to nitrocellulose membrane (Bio-Rad Laboratories). Primary antibodies used included anti-STMN1 (1:1000 dilution), anti-PARP (1:1000 dilution) (Cell Signaling Technology, Beverly, MA, USA), anti-GAPDH (1:10,000 dilution) (Millipore Corp., Bedford, MA, USA). After incubation with peroxidase conjugated secondary antibody (1:10,000 dilution for anti-GAPDH; 1:2000 for other primary antibodies) (Santa Cruz Biotechnology, Heidelberg, Germany), protein expression was detected using SuperSignal West Pico Chemiluminescent Substrate (Thermo Scientific, Rockford, IL, USA).

SK-HEP-1/Luc$^+$ xenograft model. SK-HEP-1 luciferase stable clone was prepared by transfecting SK-HEP-1 cells with firefly luciferase expression vector and selected with 500 μg/ml Geneticin (Gibco-BRL) for 4 weeks. Individual colonies were screened for bioluminescence activity using the Xenogen IVIS® imager (Alameda, CA, USA). Clones with stable luminescence expression were used for *in vivo* studies.

Male BALB/c nude mice at 6-8 weeks old with an average body weight of ~20 g were anesthetized by intraperitoneal injection of ketamine hydrochloride (120 mg/kg) (Fort Dodge Animal Health, Fort Dodge, IA, USA) plus xylazine (6 mg/kg) (Phoenix Scientific, Inc., St. Joseph, MO, USA). Anesthetized animals then received $5x10^6$ SK-HEP-1/Luc$^+$ cells suspended in 200 μl serum-free medium by subcutaneous injection below the dorsal flank. Drug treatments started on day 14 after tumor cells inoculation. Mice were divided into 5 groups: PBS (n=13), *nab*-paclitaxel (n=14), paclitaxel (n=9), docetaxel (n=9) and doxorubicin, (n=10). Based on the suggested dose of 30 mg/kg (35 mmol/kg) *nab*-paclitaxel in a previous study on multiple cancers, all drugs were given every two days for five times, at a dose of 35 mmol/kg (*nab*-paclitaxel: 30 mg/kg, paclitaxel: 30 mg/kg, docetaxel: 28 mg/kg, doxorubicin: 19 mg/kg) (22). Tumor growth was monitored twice weekly by *in vivo* bioluminescent imaging and by external caliper measurements using the formula of [(length x width^2)/2] for 24 days. For *in vivo* bioluminescent imaging, 150 mg/kg D-luciferin were given by intraperitoneal injection and 10 min after luciferin injection, mice were anesthetized by isoflurane and tumor cell viability was measured by the Xenogen IVIS

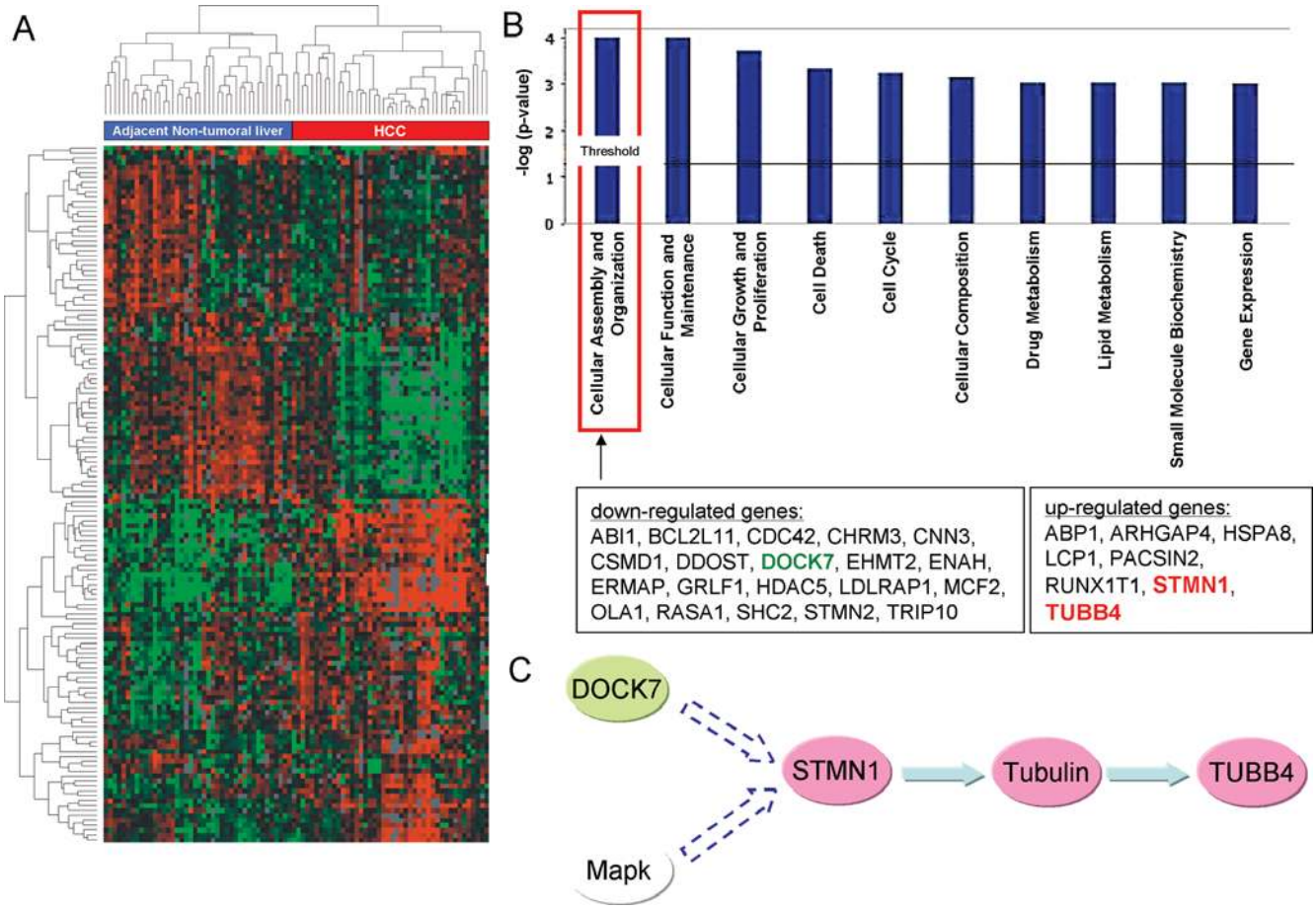

Figure 1. (A) Gene expression patterns were identified in 43 paired HCC tumors and adjacent non-tumoral livers. The top 649 genes (fold change >2.0) are illustrated. Relative gene expression is color coded in which red represents high relative expression and green represents low relative expression in HCC tumors compared with adjacent non-tumoral livers. Patients are identified in the dendrogram across the top, whereas genes are represented by the dendrogram on the left. (B) Ingenuity Pathway Analysis revealed 10 top ranked functional ontologies in HCC. The up-regulated and down-regulated genes involved in cellular assembly and organization are shown. (C) The STMN1-tubulin axis path is illustrated. Red color represents genes that are up-regulated, while green color denotes down-regulated genes.

imager. Experimental protocols and procedures were approved by the Animal Research Ethics committee of the Chinese University of Hong Kong.

Statistical analysis. The data are presented as mean ± SD. Student's t-test, Kaplan-Meier survival curves and One-way ANOVA analysis were performed using Graphpad Prism 3.0 software. Differences were considered statistically significant at $P<0.05$.

Results

Functional ontologies involved in HCC development. To facilitate biological interpretation of Gene Ontologies in the development of HCC, genes from our microarray dataset were first ranked and selected by evidence of significant differential expression according to statistical methods described in the Materials and methods. Enriched differential expressed genes obtained from SAM and Wilcoxon signed rank test were expected to be more robust that changing thresholds alone, and were subjected to analysis for functional networks involved present. The heat map diagram (Fig. 1A) illustrates the pattern of clustering across patient samples and genes. IPA analysis of ~1,000 significant known genes (top 5% percentile changes) suggested a few significant gene ontologies, which included cellular assembly and organization, cellular function and maintenance, cell death, cell cycle, cellular composition, drug and lipid metabolism and small molecules biochemistry (Fig. 1B). In particular, the cellular assembly and organization category ranked the most significant event, where over-representations of microtubule associated genes such as STMN1 and TUBB4 were found (Fig. 1C).

Cytotoxic effect of taxanes on HCC cells. We first evaluated the effect of microtubule targeting drugs, paclitaxel, docetaxel and *nab*-paclitaxel, on HCC cell lines that displayed elevated STMN1 expressions, which would infer the presence of deregulated microtubule organization (Fig. 2B). A high sensitivity towards the taxane-based drugs was generally found in Hep3B, SK-HEP-1 and HKCI-9 compared to doxorubicin, a chemotherapeutic agent that is widely used for many cancers, including HCC (Fig. 2A). Remarkably, *nab*-paclitaxel showed the highest potency with a lowest effective dosage found in

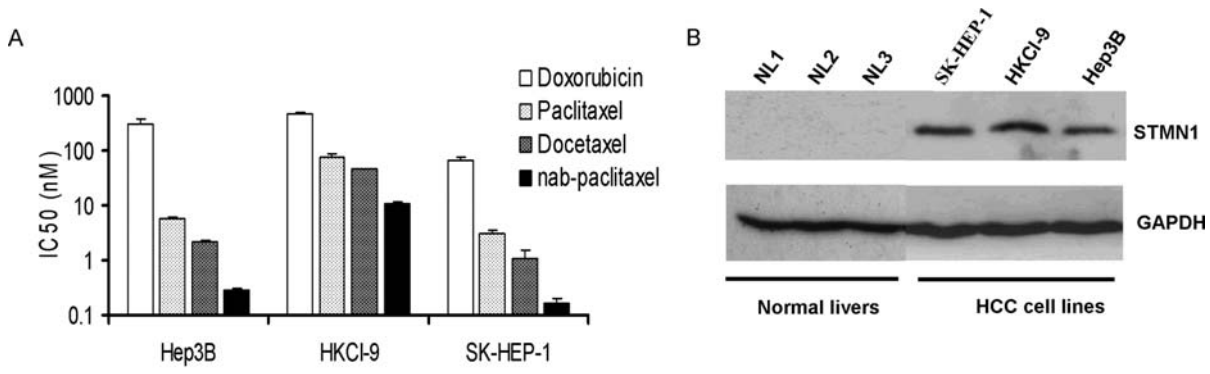

C

Drugs (IC50, nM)	Hep3B	HKCI-9	SK-HEP-1
doxorubicin	314.03±74.46	455.93±35.72	67.25±2.40
paclitaxel	5.80±0.33	74.22±10.05	3.16±0.45
docetaxel	2.10±0.20	45.00±1.54	1.11±0.14
nab-paclitaxel	0.29±0.02	10.42±1.37	0.16±0.05
Fold Change (doxorubicin vs nab-paclitaxel)	1082	44	420

Figure 2. (A) Cytotoxic effects of taxanes and doxorubicin in HCC. Cell lines Hep3B, HKCl-9 and SK-HEP-1 were treated with increasing concentrations of doxorubicin, paclitaxel, docetaxel, and *nab*-paclitaxel for 48 h. Effect on cell viability was investigated by MTT, and the IC_{50} values determined. Experiments were repeated three times and expressed as the mean ± SD. (B) The expression of STMN1 in normal livers and HCC cell lines as detected by Western blotting. (C) The IC_{50} value of drugs tested in HCC cell lines listed.

all 3 cell lines tested. The IC_{50} obtained on *nab*-paclitaxel ranged from 0.29±0.02 to 10.42±1.37 nM, which was about 44-1082-fold less than doxorubicin (IC_{50} value ranged from 105.95±10.58 to 455.93±35.72 nM) and 7-20 fold less than standard paclitaxel (IC_{50}value ranged from 3.16±0.45 nM to 74.22±10.05 nM) (Fig. 2C).

nab-paclitaxel treatment induced cell cycle blockade and apoptosis. It is known that paclitaxel induces mitotic arrest through stabilizing microtubule polymerization (26,27). We observed a similar effect with *nab*-paclitaxel, where a higher degree of microtubule polymerization was found in the treated cells (Fig. 3). The effect of *nab*-paclitaxel on the cell cycle was also studied. In both Hep3B and SK-HEP-1, flow cytometric analysis indicated that an increase in the G_2/M population was found with increasing concentrations of *nab*-paclitaxel applied, suggesting a dose-dependent cell cycle arrest ($P<0.05$; Fig. 4B). Flow cytometry profile also showed a sub-G_1 fraction appearing after the treatment with *nab*-paclitaxel (Fig. 4A). The presence of apoptotic cells were further confirmed in SK-HEP-1 and Hep3B by TUNEL analysis, which indicated the number of TUNEL positive cells corresponded to the amount of *nab*-paclitaxel used ($P<0.001$; Fig. 4C and D). The cleavage of nuclear protein PARP was determined by monitoring the presence of 89 kDa cleaved product. PARP cleavage became evident at 12 h after treatment and gradually increased over 48 h (Fig. 4E).

Effect of nab-paclitaxel on in vivo xenograft growth. We subcutaneously injected SK-HEP-1/Luc$^+$ cells into BALB/c nude mice and examined the anti-tumoral effects of taxanes and doxorubicin *in vivo*. Developed xenograft was measured for tumor size on the first day of treatment and twice weekly thereafter by IVIS imaging and caliper measurements. Fig. 5A shows the percentage change of tumor size in each treatment group with time. The control PBS group showed a gradual increase in tumor size over the period of study. While each treatment group showed a reduction in tumor size, the toxicities from doxorubicin, paclitaxel and docetaxel were particularly severe, which resulted in much weight loss and deaths of many mice within 3 injections (Fig. 5B and C). Although weight loss was also observed with *nab*-paclitaxel injection, it was least severe and the mice were generally able to re-gain body weight after the last injection on day 9. The anti-tumoral effect of *nab*-paclitaxel was highly significant with considerable inhibition on tumor sizes compared to control group ($P=0.0007$). Moreover, >60% of mice survived to the end of experiments (Fig. 5B).

STMN1 knockdown increases sensitivity to taxane drugs. Silencing of STMN1 has been shown to promote microtubule polymerization (28). We hence sought to examine the possible synergistic effect of STMN1 knockdown and microtubule stabilizing drugs in HCC. Fig. 6A showed the STMN1 protein level in Hep3B after siRNA knockdown on days 1 and 3.

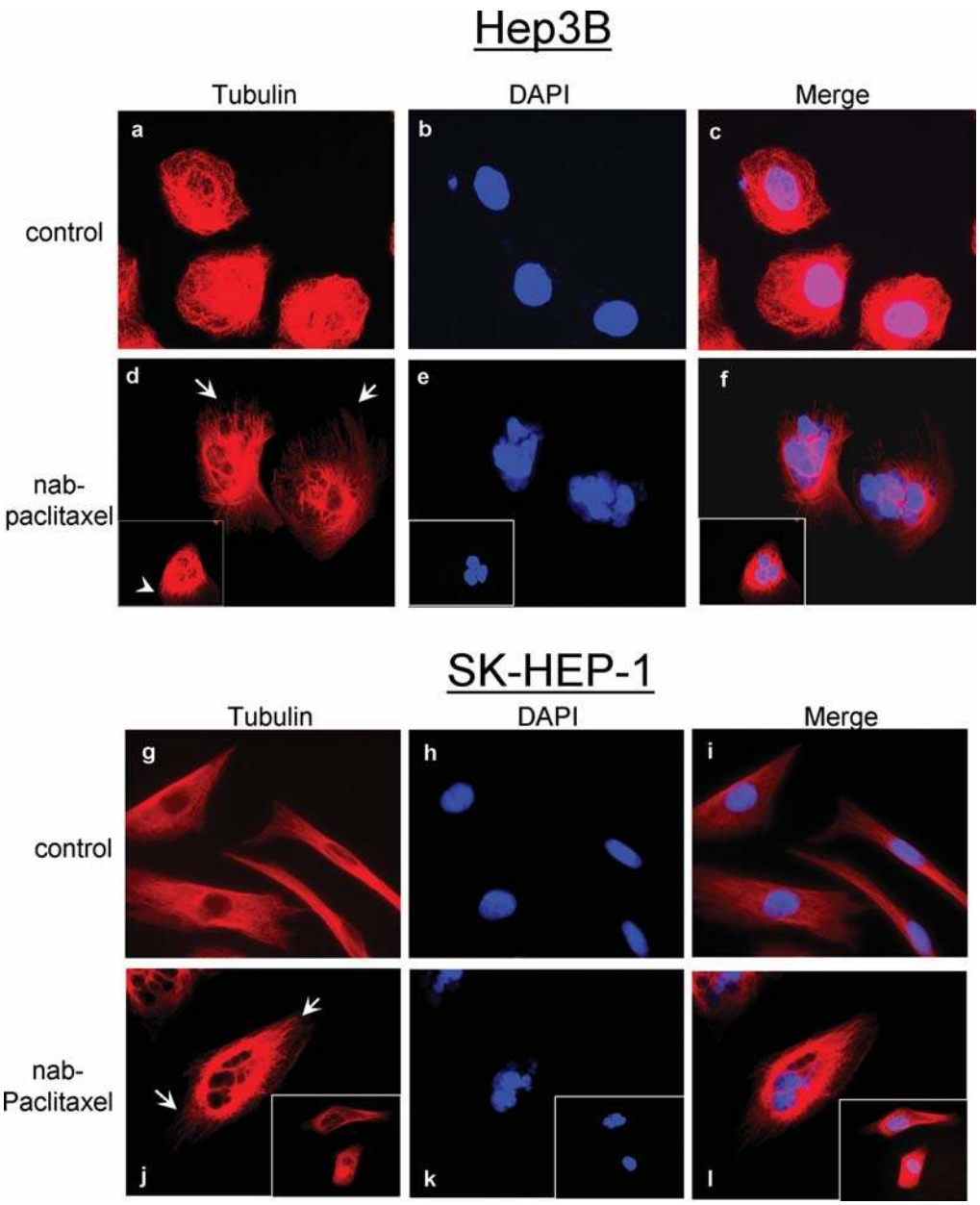

Figure 3. Microtubule morphology in Hep3B and SK-HEP-1 cells treated with *nab*-paclitaxel. Cells treated with 5 ng/ml *nab*-paclitaxel for 24 h were fixed in 4% paraformaldehyde, and stained for ß-tubulin (red). Nuclei were counterstained with DAPI (blue). (a-c), Hep3B control; (d-f), *nab*-paclitaxel treated Hep3B. (g-i), SK-HEP-1 control; (j-l), *nab*-paclitaxel treated SK-HEP-1. Inserts in figures (d-f) and (j-l) are captures from a different field from the same slide. *nab*-paclitaxel treated cells showed a higher degree of microtubule polymerization (arrows). Representative images from two independent experiments are shown.

Specific STMN1 knockdown in Hep3B showed ~40% decrease in cell viability compared to mock on day 3 post-transfection (Fig. 6B). In the combinatory study with taxanes, Hep3B transfected with siSTMN1 was 7.7-fold more sensitive to *nab*-paclitaxel (IC_{50}, 0.04±0.004 vs 0.31±0.04 nM) and 2.7-fold more sensitive to paclitaxel (IC_{50}, 1.95±0.28 vs 5.17±0.06 nM) (Fig. 6C). In contrast, knockdown of STMN1 had no effect on the sensitivity of doxorubicin, a drug that does not target the microtubules.

Discussion

In this study, we performed microarray profiling for paired HCC tumors and adjacent non-tumoral livers in an effort to define deregulated functional ontologies that are associated with the development of HCC. Enriched differential expressed genes obtained from SAM and Wilcoxon signed rank test were subjected to pathway analysis using IPA. Using this approach, we found that the cellular assembly and organization through the microtubule functional networks ranked the most significant cellular event in HCC. Our finding is consistent with several earlier reports on expression profiling of HCC, which also suggested the microtubule-based processes and microtubule cytoskeletal organization to be important biological and cellular components in HCC (29,30). In line with our finding, other profiling studies also found the microtubule regulatory gene STMN1 to be commonly up-regulated in HCC (31,32). Collectively, these investigations

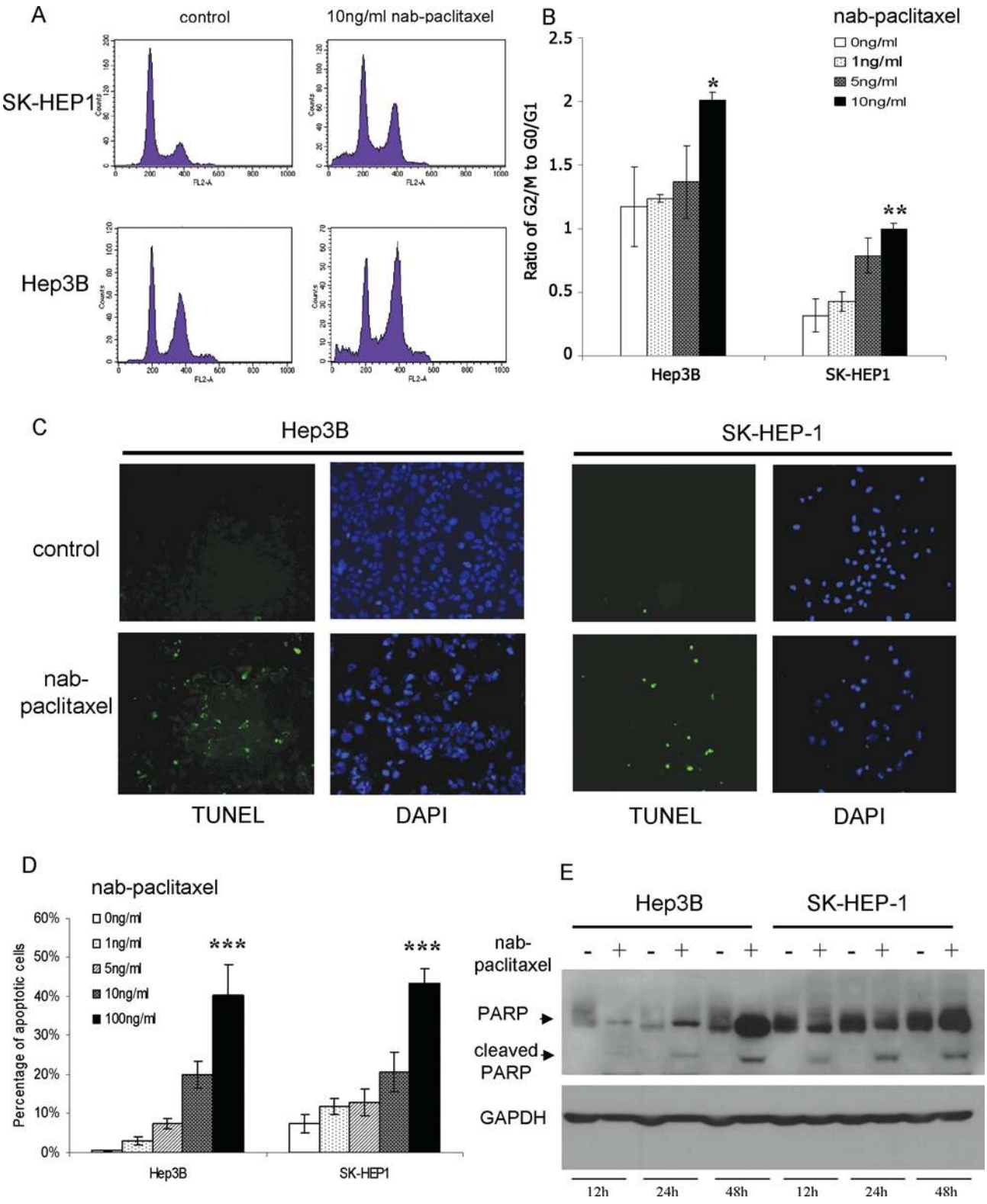

Figure 4. (A) Cell cycle profile of *nab*-paclitaxel treated Hep3B and SK-HEP-1. Cells treated with differing concentrations of *nab*-paclitaxel for 12 h were harvested, stained with PI, and analyzed by flow cytometry. (B) Ratio of G_2M to G_0/G_1 populations in Hep3B and SK-HEP-1 in response to varying concentrations of *nab*-paclitaxel. $^{*}P<0.05$, $^{**}P<0.01$ (One-way ANOVA). (C) TUNEL analysis in Hep3B and SK-HEP-1 cells showed increase number in apoptotic cells (green) after treatment of *nab*-paclitaxel at 100 ng/ml for 48 h. Nuclei counterstained with DAPI. Images shown are representative of two independent experiments. (D) Percentage of apoptotic cells increased with increasing concentrations of *nab*-paclitaxel applied. $^{*}P<0.05$, $^{**}P<0.01$ (One-way ANOVA). (E) Western blotting for PARP in Hep3B and SK-HEP-1 treated with *nab*-paclitaxel showed increasing amount of cleaved PARP with time.

provide a rationale for targeting the microtubules in HCC. However, to our knowledge, only a few studies have reported on the use of anti-microtubule agents as a therapeutic strategy in HCC (33,34). In this study, we hence examined the microtubule stabilizing taxanes for their effects in preclinical models of HCC.

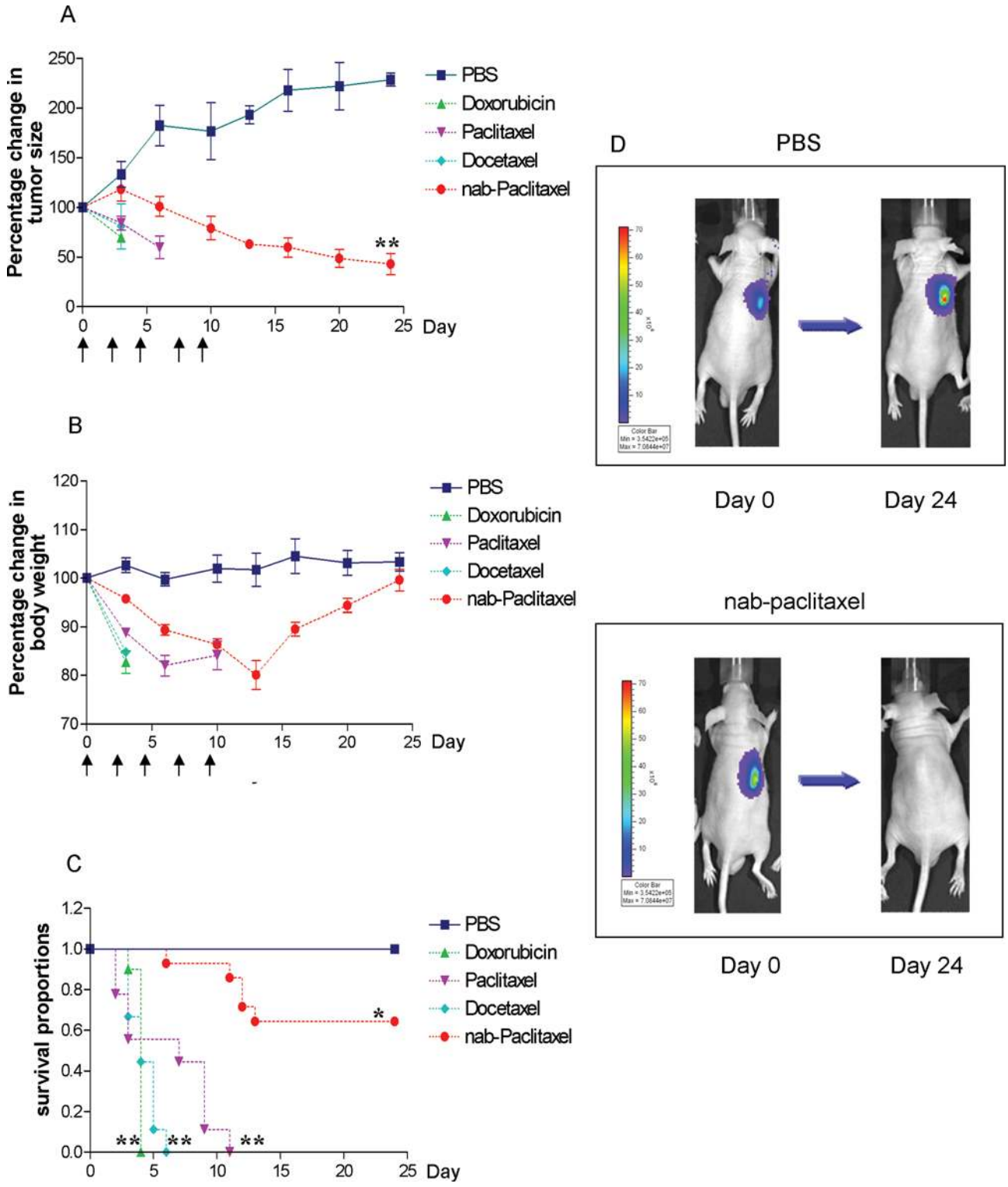

Figure 5. Effect of *nab*-paclitaxel on HCC tumor growth *in vivo*. SK-HEP-1/Luc$^+$ cells (5x10^6) were injected subcutaneously into male BALB/c nude mice (n=9-13 for each group). Two weeks after tumor inoculation, mice received intraperitoneal injection of drugs (35 mmol/kg) every two days, five times. (A) Tumor growth was monitored and quantified twice weekly. A significant difference between the vehicle group and *nab*-paclitaxel treated group was observed at the end of observation (paired t-test, **P<0.01 compared to PBS group). Animals on other treatment groups died within 3 injections. Arrows indicate time of drug injection. (B) Percentage change in body weight of mice from drug treatments. (C) Survival curve was plotted according to the status of the mice during experiments. A significant difference between the vehicle group and drug treated groups was observed (*P<0.05, **P<0.01, compared to PBS group). (D) IVIS images of representative mice of control and *nab*-paclitaxel treated are shown.

Taxanes are known to bind microtubules polymers and stabilize microtubule in tumor cells, thereby arrest cells in G_2/M and promote cell death by suppressing microtubule dynamics (15,35). Paclitaxel and docetaxel have shown significant clinical activities in various solid tumors, such as breast, ovarian, and prostate cancers; and effectiveness in

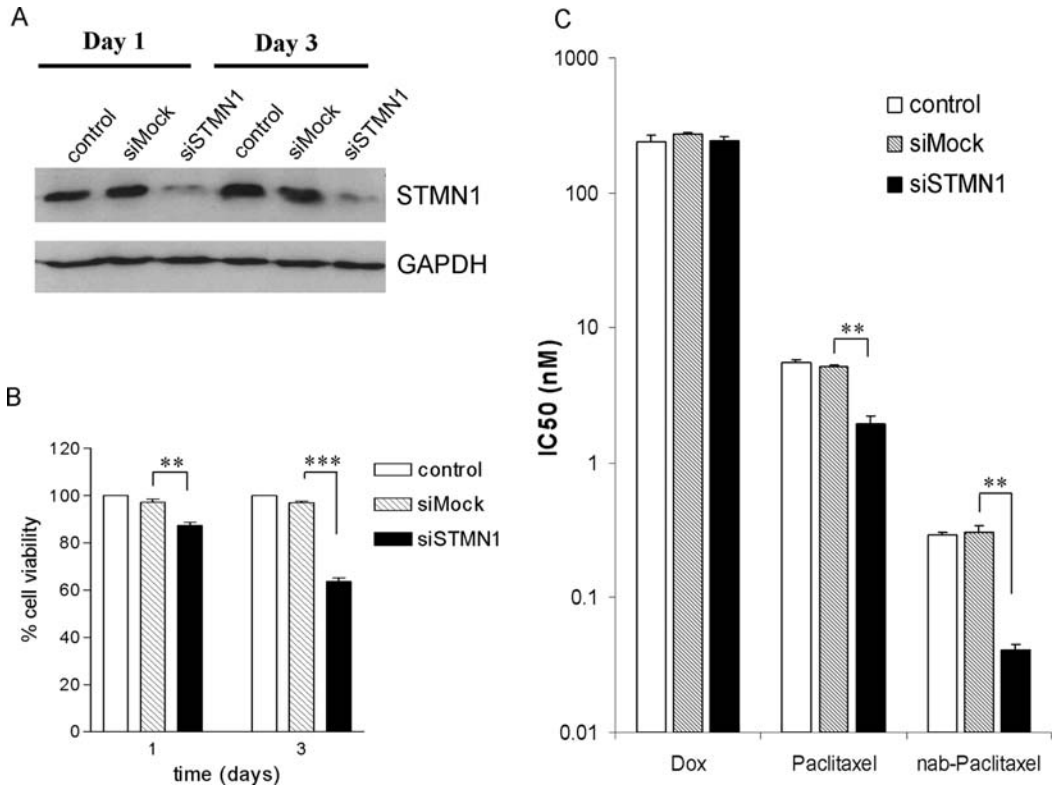

Figure 6. Effect on drug sensitivity following silencing of STMN1 gene expression. (A) Level of STMN1 at days 1 and 3 after siRNA knockdown. STMN1 expression was determined by Western blotting. Images are representative of three independent experiments. (B) Silencing of STMN1 inhibits Hep3B cell viability by ~40% on day 3. Data are expressed as means ± SD of three independent experiments (**P<0.01, ***P<0.001 compared to siMock group). (C) Silencing of STMN1 expression sensitized STMN1-overexpressing cells to anti-microtubule drugs. Hep3B cells transfected with siSTMN1 were treated with doxorubicin, paclitaxel and *nab*-paclitaxel for 48 h. Distinct synergistic effect was suggested with *nab*-paclitaxel. Results shown represent mean ± SD from 2 or more independent experiments (*P<0.05, **P<0.01 compared to siMock group).

pre-clinical study models of non-small cell lung cancer, head and neck cancer, and esophageal cancer (16-18). Because of their low aqueous solubility, organic vehicles such as polyoxyethylated castor oil (Cremophor EL), polysorbate 80 (Tween-80) and ethanol have been used to formulate these drugs, but these solvents are also directly associated with severe toxicity and hypersensitivity reactions (19,20). Pre-medication of steroid and anti-histamine is required to minimize the risk of hypersensitivity reaction but severe or even fatal hypersensitivity reaction still occurs (35,36). Such undesirable side effects have in part rendered few clinical studies in the use of taxanes in HCC patients. The lyophilized formulation of *nab*-paclitaxel comprising of albumin and paclitaxel is reconstituted in 0.9% NaCl and forms a colloidal suspension during administration. Because of its formulation, which is devoid of any solvents or ethanol (21), *nab*-paclitaxel has much less treatment-related toxicity. In comparing the effects and toxicity of paclitaxel and docetaxel with *nab*-paclitaxel, our study showed that paclitaxel and docetaxel were more effective than doxorubicin, although *nab*-paclitaxel exhibited the highest efficacy in inhibiting HCC cell viability with the lowest IC_{50} consistently determined in HCC cell lines. *nab*-paclitaxel induced G_2/M arrest through microtubule polymerization that concluded in apoptosis. In our *in vivo* animal study, we have used an equivalent molar concentration of *nab*-paclitaxel along with paclitaxel, docetaxel and doxorubicin. Our data suggested that *nab*-paclitaxel is the most effective cytotoxic agent with maximum tolerance in xenograft model.

In defining the cellular assembly network in HCC, we also found the microtubule regulatory gene *STMN1* to be significantly over-expressed. It is a microtubule-destabilizing factor that plays an important role in controlling cellular proliferation by promoting microtubule depolymerization (37-40). Over-expression of STMN1 has been reported for various types of tumor such as leukemia, breast cancer, ovarian cancer and HCC (41-43). As STMN1 is a microtubule-destabilizing factor, we examined if knockdown STMN1 expression could provide a synergistic effect with *nab*-paclitaxel treatment in HCC. Knockdown of STMN1 expression readily reduced cell viability by about 40% in Hep3B. More significantly, suppression of STMN1 could sensitize HCC cells to *nab*-paclitaxel by ~8-fold. In line with our finding, Alli *et al* demonstrated that STMN1 over-expression reduced sensitivity to paclitaxel treatment in breast cancer cell line (44). Nevertheless, knockdown of STMN1 did not seem to have altered sensitivity of HCC cells to doxorubicin, which is mainly a DNA-targeting drug. These results implied that treatment strategy targeting both microtubule and STMN1 could enhance therapeutic effects on HCC cells. In this context, the specific reduction of STMN1 expression, for example, by small molecules that inhibit STMN1 bioactivity or ribozyme-mediated knockdown

approaches, may offer novel therapeutic options for HCC patients. Recently, it was reported that STMN1 might be a molecular target of two xanthones, gambogic acid and gambogenic acid (45). The use of *nab*-paclitaxel alone or in combination treatment using gambogic acid or gambogenic acid may hold promises as novel treatment options in HCC patients and warrants for further clinical investigations.

Acknowledgments

This work was supported by a Collaborative Research Fund from the Hong Kong Research Grants Council (Ref. No.: CUHK4/CRF/08), a CUHK Direct Grant for Research Project Code: 2041338 and a grant from the NIH, USA (Ref. No.: ES006096). The authors thank Dr C.C. Holmes (University of Oxford, UK) for bioinformatic support, and Dr K.Y. Chan and Ms. N.L. Wong for technical assistance.

References

1. Parkin DM: Global cancer statistics in the year 2000. Lancet Oncol 2: 533-543, 2001.
2. Yeo W, Mok TS, Zee B, *et al*: A randomized phase III study of doxorubicin versus cisplatin/interferon alpha-2b/doxorubicin/fluorouracil (PIAF) combination chemotherapy for unresectable hepatocellular carcinoma. J Natl Cancer Inst 97: 1532-1538, 2005.
3. Gish RG, Porta C, Lazar L, *et al*: Phase III randomized controlled trial comparing the survival of patients with unresectable hepatocellular carcinoma treated with nolatrexed or doxorubicin. J Clin Oncol 25: 3069-3075, 2007.
4. Ramanathan RK, Belani CP, Singh DA, *et al*: Phase II study of lapatinib, a dual inhibitor of epidermal growth factor receptor (EGFR) tyrosine kinase 1 and 2 (Her2/Neu) in patients (pts) with advanced biliary tree cancer (BTC) or hepatocellular cancer (HCC). A California Consortium (CCC-P) Trial. J Clin Oncol 24: 4010, 2006.
5. O'Dwyer PJ, Giantonio BJ, Levy DE, Kauh JS, Fitzgerald DB and Benson AB: Gefitinib in advanced unresectable hepatocellular carcinoma: results from the Eastern Cooperative Oncology Group's Study E1203. J Clin Oncol 24: 4143, 2006.
6. Cheng AL, Kang YK, Chen ZD, *et al*: Efficacy and safety of sorafenib in patients in the Asia-Pacific region with advanced hepatocellular carcinoma: a phase III randomised, double-blind, placebo-controlled trial. Lancet Oncol 10: 25-34, 2009.
7. Ng IOL, Liu CL, Fan ST and Ng M: Expression of P-glycoprotein in hepatocellular carcinoma - a determinant of chemotherapy response. Am J Clin Pathol 113: 355-363, 2000.
8. Endicott JA and Ling V: The biochemistry of P-glycoprotein-mediated multidrug resistance. Annu Rev Biochem 58: 137-171, 1989.
9. Park JG, Lee SK, Hong IG, *et al*: Mdr1 gene-expression - its effect on drug-resistance to doxorubicin in human hepatocellular-carcinoma cell-lines. J Natl Cancer Inst 86: 700-705, 1994.
10. Yokoe T, Tanaka F, Mimori K, Inoue H, Ohmachi T, Kusunoki M and Mori M: Efficient identification of a novel cancer/testis antigen for immunotherapy using three-step microarray analysis. Cancer Res 68: 1074-1082, 2008.
11. Bergamaschi A, Hjortland GO, Triulzi T, *et al*: Molecular profiling and characterization of luminal-like and basal-like *in vivo* breast cancer xenograft models. Mol Oncol 3: 469-482, 2009.
12. Zagani R, Hamzaoui N, Cacheux W, *et al*: Cyclooxygenase-2 inhibitors down-regulate osteopontin and Nr4a2-new therapeutic targets for colorectal cancers. Gastroenterology 137: 1358-1366, 2009.
13. Goto Y, Matsuzaki Y, Kurihara S, *et al*: A new melanoma antigen fatty acid-binding protein 7, involved in proliferation and invasion, is a potential target for immunotherapy and molecular target therapy. Cancer Res 66: 4443-4449, 2006.
14. Scrideli CA, Carlotti CG, Okamoto OK, *et al*: Gene expression profile analysis of primary glioblastomas and non-neoplastic brain tissue: identification of potential target genes by oligonucleotide microarray and real-time quantitative PCR. J Neurooncol 88: 281-291, 2008.
15. Nogales E, Wolf SG and Downing KH: Structure of the alpha beta tubulin dimer by electron crystallography. Nature 391: 199-203, 1998.
16. Rowinsky EK: The development and clinical utility of the taxane class of antimicrotubule chemotherapy agents. Annu Rev Med 48: 353-374, 1997.
17. Gan YB, Wientjes MG, Schuller DE and Au JLS: Pharmacodynamics of taxol in human head and neck tumors. Cancer Res 56: 2086-2093, 1996.
18. Yen WC, Wientjes MG and Au JLS: Differential effect of taxol in rat primary and metastatic prostate tumors: Site-dependent pharmacodynamics. Pharmaceut Res 13: 1305-1312, 1996.
19. Szebeni J, Alving CR, Savay S, Barenholz Y, Priev A, Danino D and Talmon Y: Formation of complement-activating particles in aqueous solutions of Taxol: possible role in hypersensitivity reactions. Int Immunopharmacol 1: 721-735, 2001.
20. Gelderblom H, Verweij J, Nooter K and Sparreboom A: Cremophor EL: the drawbacks and advantages of vehicle selection for drug formulation. Eur J Cancer 37: 1590-1598, 2001.
21. Green MR, Manikhas GM, Orlov S, Afanasyev B, Makhson AM, Bhar P and Hawkins MJ: Abraxane((R)), a novel Cremophor((R))-free, albumin-bound particle form of paclitaxel for the treatment of advanced non-small-cell lung cancer. Ann Oncol 17: 1263-1268, 2006.
22. Desai N, Trieu V, Yao ZW, *et al*: Increased antitumor activity, intratumor paclitaxel concentrations, and endothelial cell transport of Cremophor-free, albumin-bound paclitaxel, ABI-007, compared with Cremophor-based paclitaxel. Clin Cancer Res 12: 1317-1324, 2006.
23. Desai NP, Trieu V, Hwang LY, Wu RJ, Soon-Shiong P and Gradishar WJ: Improved effectiveness of nanoparticle albumin-bound (*nab*) paclitaxel versus polysorbate-based docetaxel in multiple xenografts as a function of HER2 and SPARC status. Anticancer Drugs 19: 899-909, 2008.
24. Wong N, Chan KYY, Macgregor PF, *et al*: Transcriptional profiling identifies gene expression changes associated with IFN-alpha tolerance in hepatitis C-related hepatocellular carcinoma cells. Clin Cancer Res 11: 1319-1326, 2005.
25. Chan KYY, Lai PBS, Squire JA, Beheshti B, Wong NLY, Sy SMH and Wong N: Positional expression profiling indicates candidate genes in deletion hotspots of hepatocellular carcinoma. Mod Pathol 19: 1546-1554, 2006.
26. Milross CG, Mason KA, Hunter NR, Chung WK, Peters LJ and Milas L: Relationship of mitotic arrest and apoptosis to antitumor effect of paclitaxel. J Natl Cancer Inst 88: 1308-1314, 1996.
27. Fan WM: Possible mechanisms of paclitaxel-induced apoptosis. Biochem Pharmacol 57: 1215-1221, 1999.
28. Alli E, Yang JM and Hait WN: Silencing of stathmin induces tumor-suppressor function in breast cancer cell lines harboring mutant p53. Oncogene 26: 1003-1012, 2007.
29. Patil MA, Chua MS, Pan KH, *et al*: An integrated data analysis approach to characterize genes highly expressed in hepatocellular carcinoma. Oncogene 24: 3737-3747, 2005.
30. Tung CY, Jen CH, Hsu MT, Wang HW and Lin CH: A novel regulatory event-based gene set analysis method for exploring global functional changes in heterogeneous genomic data sets. BMC Genom 10: 26, 2009.
31. Breuhahn K, Vreden S, Haddad R, *et al*: Molecular profiling of human hepatocellular carcinoma defines mutually exclusive interferon regulation and insulin-like growth factor II over-expression. Cancer Res 64: 6058-6064, 2004.
32. Wang W, Peng JX, Yang JQ and Yang LY: Identification of gene expression profiling in hepatocellular carcinoma using cDNA microarrays. Dig Dis Sci (In press).
33. Mok TSK, Choi E, Yau D, Johri A, Yeo W, Chan ATC and Wong C: Effects of patupilone (epothilone B; EPO906), a novel chemotherapeutic agent, in hepatocellular carcinoma: an *in vitro* study. Oncology 71: 292-296, 2006.
34. Nimeiri HS, Singh DA, Kasza K, Taber DA, Ansari RH, Vokes EE and Kinder HL: The epothilone B analogue ixabepilone in patients with advanced hepatobiliary cancers: a trial of the University of Chicago Phase II Consortium. Invest New Drugs (In press).
35. Schiff PB and Horwitz SB: Taxol stabilizes microtubules in mouse fibroblast cells. Proc Natl Acad Sci USA Biol Sci 77: 1561-1565, 1980.

36. Kloover JS, den Bakker MA, Gelderblom H and van Meerbeeck JP: Fatal outcome of a hypersensitivity reaction to paclitaxel: a critical review of premedication regimens. Br J Cancer 90: 304-305, 2004.
37. Belmont LD and Mitchison TJ: Identification of a protein that interacts with tubulin dimers and increases the catastrophe rate of microtubules. Cell 84: 623-631, 1996.
38. Mistry SJ and Atweh GF: Stathmin inhibition enhances okadaic acid-induced mitotic arrest - a potential role for stathmin in mitotic exit. J Biol Chem 276: 31209-31215, 2001.
39. Marklund U, Larsson N, Gradin HM, Brattsand G and Gullberg M: Oncoprotein 18 is a phosphorylation-responsive regulator of microtubule dynamics. EMBO J 15: 5290-5298, 1996.
40. Mistry SJ, Li HC and Atweh GF: Role for protein phosphatases in the cell-cycle-regulated phosphorylation of stathmin. Biochem J 334: 23-29, 1998.
41. Price DK, Ball JR, Bahrani-Mostafavi Z, *et al*: The phosphoprotein Op18/stathmin is differentially expressed in ovarian cancer. Cancer Inves 18: 722-730, 2000.
42. Bieche I, Lachkar S, Becette V, Cifuentes-Diaz C, Sobel A, Lidereau R and Curmi PA: Overexpression of the stathmin gene in a subset of human breast cancer. Br J Cancer 78: 701-709, 1998.
43. Daibata M, Matsuo Y, Machida H, Taguchi T, Ohtsuki Y and Taguchi H: Differential gene-expression profiling in the leukemia cell lines derived from indolent and aggressive phases of CD56(+) T-cell large granular lymphocyte leukemia. Int J Cancer 108: 845-851, 2004.
44. Alli E, Bash-Babula J, Yang JM and Hait WN: Effect of stathmin on the sensitivity to antimicrotubule drugs in human breast cancer. Cancer Res 62: 6864-6869, 2002.
45. Wang X, Chen YC, Han QB, *et al*: Proteomic identification of molecular targets of gambogic acid: Role of stathmin in hepatocellular carcinoma. Proteomics 9: 242-253, 2009.